

## MICRO PROJECTION LITHOGRAPHY INSIDE DEEP TRENCHES USING MICROLENS ON A MASK

Chang-Hyeon Ji\*, Florian Herrault, and Mark G. Allen  
Georgia Institute of Technology, Atlanta, Georgia, U. S. A.

### ABSTRACT

This paper presents a micro projection lithography process which enables the patterning of photoresist at the bottom surface of deep cavities, using microlenses formed directly on the mask. Arrays of cylindrical plano-convex microlenses on conventional photomasks have been fabricated by a photoresist melting and reflow technique, thereby augmenting the proximity lithography performance of these masks. Patterning results inside deep trenches have been analyzed. A maximum pattern width reduction of 64% for a 60 $\mu\text{m}$  rectangular pattern at the bottom of a 216 $\mu\text{m}$ -deep trench has been achieved with a microlens with a focal length of 267 $\mu\text{m}$ . The effect of the focal length variation on the pattern size variation has been analyzed.

### KEYWORDS

Microlens, Projection lithography, Three-dimensional packaging

### INTRODUCTION

As a recently highlighted technology for the semiconductor and MEMS industry, three-dimensional packaging often involves patterning on substrates with extreme topographies up to hundreds of microns deep (Figure 1(b)) [1]. Previously we have reported a through-wafer interconnection technology based on electroplated buried metal interconnects formed at the bottom surface of 300 $\mu\text{m}$ -deep trenches [2]. Although patterning of spray coated photoresist inside deep-etched vertical trenches has been implemented successfully, the issue of pattern size control still remains. While patterns as small as 10 $\mu\text{m}$  at the bottom of 100 $\mu\text{m}$ -deep tapered vias have been obtained by conventional lithography processes for certain applications [3], difficulties with proximity patterning increase as the depth and complexity of the trench (via) geometry increase. The uniformity of the photoresist spray coated on a high topography surface depends on the trench opening size and depth, and some of the patterns have to be over-exposed to fully define patterns with different sizes.

To overcome the pattern size increase resulting from the significant gap between the mask and photoresist (proximity effect), we have locally formed cylindrical plano-convex microlenses on the chromium surface of the mask by a photoresist reflow technique (Figure 1(c)) [4]. The patterned chromium layer on the mask works as a field stop for the fabricated microlenses. Although various types of microlens arrays have been utilized in photolithography

process for large area proximity printing [5], and for generation of an array of projection-reduced patterns [6], patterning on severe topographies with a lensed mask has not been explored. Using this simple photomask modification technique, patterns even smaller than the original size on the mask can be generated without having to resort to exposure tools with projection capability. Moreover, simultaneous exposure and pattern generation on top and bottom of high topography surfaces can benefit from the proposed fabrication approach.

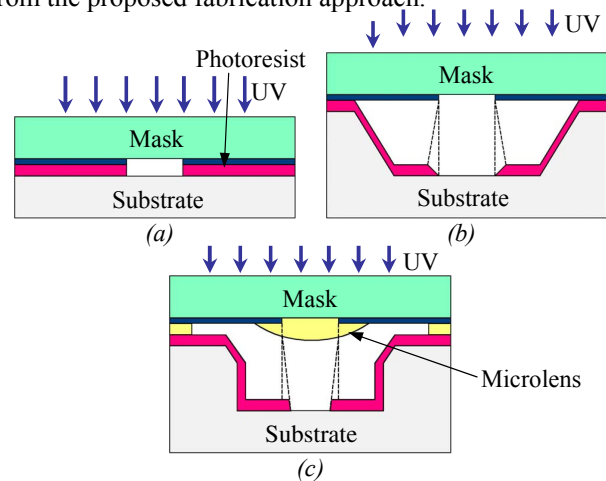


Figure 1: Micro projection lithography concept; (a) conventional contact exposure, (b) proximity exposure inside deep trench, (c) this work

### MICROLENS DESIGN AND FABRICATION

To verify the concept, microlenses with two different initial photoresist thicknesses ( $T_i$ , 13.7 and 26.3 $\mu\text{m}$ ) have been fabricated and tested (Figure 2). For the fabrication of microlenses, positive-tone photoresist (Clariant, AZ P4620) has been spin-coated on the chromium side of the 4-inch mask plate with a one-dimensional array of via patterns. Photoresist has been patterned to form a rectangular pedestal long enough to fully cover the array of vias, and heat treated on a hot plate for melting and reflow to form cylindrical plano-convex lens, as detailed in Table 1.

Table 1: Process conditions and characteristics of the microlens

	$T_i$ [ $\mu\text{m}$ ]	Spin speed [rpm] / Time [sec]	Heat treatment	Transmittance (405nm) [%]
Mask #1	13.7	1,000 / 35	30min@ 150°C	52.6
Mask #2	26.3	500 / 35	ramp up and down	26.3

Theoretically, only the widths ( $x$ -axis) of the patterns are affected because of the cylindrical lens shape. To account for the decrease in mask transmittance due to microlenses, a control sample consisting of a photoresist layer of the same thickness and heat treatment condition has been formed on a blank glass substrate, and transmittance of the target ultraviolet source (405nm) has been measured (Table 1).

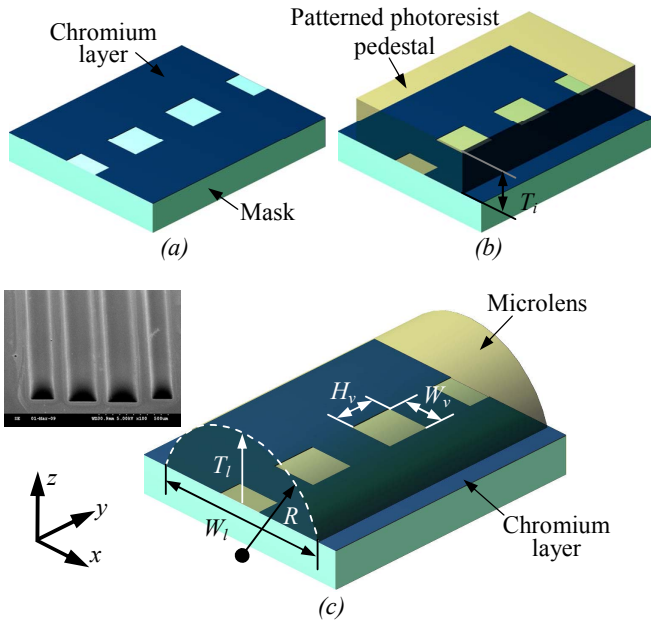


Figure 2: Schematic of the fabrication sequence; (a) mask pattern transfer, (b) photoresist patterning ( $T_i$  is the initial photoresist thickness), (c) lens shaping by melting and reflow ( $W_b$ ,  $T_b$ ,  $R$ ,  $W_v$ , and  $H_v$  are lens width, thickness, radius of curvature, via pattern width and height, respectively. Inset shows the SEM image of the fabricated microlens array.)

Figure 3 shows the profiles of the fabricated microlenses measured with white light interferometry for the estimation of focal lengths ( $f$ ). Assuming an ideal cylindrical lens shape, the focal length of a plano-convex lens can be calculated by simplified version of the lens maker's formula ( $f=R/(\mu-1)$ ), where  $\mu$  is the refractive index of the photoresist [7]. Figure 4 shows the comparison between curve fitting and analytical results for the estimation of radius of curvature. Although the discrepancy between the actual profile and the curve fitting result increases as the lens profile approaches the outer edge, utilization of the fitting result for focal length estimation remains valid as the via pattern width ( $W_v$ ) of the chromium mask is much smaller than the lens width. The chromium layer effectively acts as a field stop with via patterns centered at the center portion of the microlens. The dimensions of the lens and underlying via sizes are summarized in Table 2, where the focal lengths are calculated with radius of curvature ( $R$ ) determined by curve fitting the measured lens profile data in Figure 3. A cylindrical lens shape has been assumed and the photoresist

refractive index ( $\mu$ ) of 1.64 was used in the calculation [7]. Although thinner lenses ( $T_i=13.7\mu\text{m}$ ) with wider width ( $W_i=190, 200\mu\text{m}$ ) did not completely form spherical shapes (Figure 3(a)), focal lengths of other lenses were well distributed from  $159\mu\text{m}$  to  $459\mu\text{m}$  (Table 2). Considering the deep trench depth, and thus exposure distance, of approximately  $200\mu\text{m}$ , the effect of focal length variation on exposure distance can be thoroughly examined with the fabricated microlens arrays.

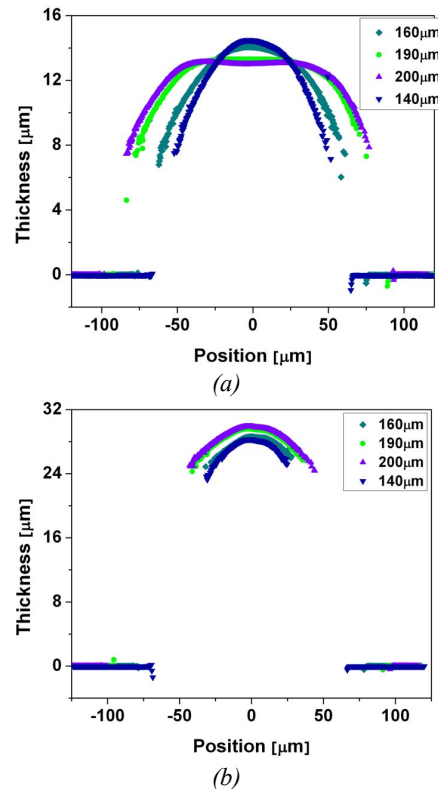


Figure 3: Measured profile of the microlens after reflow for different width ( $W_{mask}$ , pattern width in the mask); (a)  $T_i=13.7\mu\text{m}$ . Note 190 and  $200\mu\text{m}$ -wide patterns did not form cylindrical lenses, (b)  $T_i=26.3\mu\text{m}$ . All widths formed cylindrical lenses.

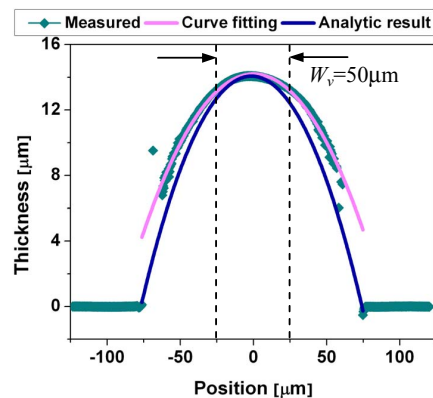


Figure 4: Measured profile of the microlens ( $W_{mask}=160\mu\text{m}$ ,  $T_i=13.7\mu\text{m}$ ) and curve fitting and analytic calculation results for radius of curvature estimation

Table 2: Dimensions of the lens and underlying via sizes defined in Figure 2

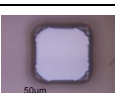
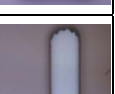
$W_v, H_v$ [ $\mu\text{m}$ ] (mask)		50	60	70	80
$W_{\text{mask}}$ [ $\mu\text{m}$ ]		160	190	200	140
Mask #1 $T_i=13.7\mu\text{m}$	$W_l$ [ $\mu\text{m}$ ]	151	181	191	131
	$T_l$ [ $\mu\text{m}$ ]	14.1	13.3	13.1	14.5
	$R$ [ $\mu\text{m}$ ]	294	N/A	N/A	197
	$f$ [ $\mu\text{m}$ ]	459	N/A	N/A	308
Mask #2 $T_i=26.3\mu\text{m}$	$W_l$ [ $\mu\text{m}$ ]	157	186	197	135
	$T_l$ [ $\mu\text{m}$ ]	28.6	29.6	29.9	28.3
	$R$ [ $\mu\text{m}$ ]	197	171	187	102
	$f$ [ $\mu\text{m}$ ]	308	267	292	159

## EXPERIMENTAL RESULTS

### Patterning on a Flat Substrate

For testing, a  $10\mu\text{m}$ -thick positive-tone photoresist (AZ P4620) has been spin-coated on a 4-inch standard silicon test wafer without trenches, and patterned with various masks and exposure methods. The gap for proximity exposure has been controlled with the aligner. An exposure dose of  $600\text{mJ}/\text{cm}^2$  has been used for all the test samples. For the mask with microlenses, the exposure dose has been adjusted to compensate for the reduced transmittance summarized in Table 1. As shown in Table 3, a pattern width ( $W_v$ ) decrease has been achieved with more reduction at shorter focal length, which validates the controlled pattern size reduction with the lensed mask. For an  $80\times 80\mu\text{m}^2$  via exposed with mask #2, the pattern was not defined correctly due to the shorter focal length ( $159\mu\text{m}$ ) compared to the exposure gap of  $200\mu\text{m}$ .

Table 3: Patterns defined with different mask and exposure method (Gap for the proximity exposure was  $200\mu\text{m}$ )

Via Size (Mask)	$50\times 50\mu\text{m}^2$	$60\times 60\mu\text{m}^2$	$70\times 70\mu\text{m}^2$	$80\times 80\mu\text{m}^2$
Hard contact				
Proximity exposure (Conventional mask)				
Proximity exposure (Mask #1)				
Proximity exposure (Mask #2)				

### Patterning inside Deep Trenches

Figure 5 shows the schematic of the fabricated deep trench and patterned photoresist at the bottom of the trench.

Using the same set of masks,  $208\text{--}217\mu\text{m}$ -deep trenches coated with spray coated photoresist have been contact exposed (Figure 1(c)), where the distance between the microlens and photoresist surface matches the trench depth ( $D_t$ ). As detailed in [2], a combined Bosch process has been developed to form deep vertical trenches with angled top-side edges, where a manual spray coating process can be applied to form patterns at the bottom of the trenches. Positive photoresist (AZ P4620) has been spray coated, and estimated thicknesses on the top and bottom surface of the trenches are  $20$  and  $5\mu\text{m}$ , respectively. As shown in Figure 6, the trenches are fully covered with excellent step and sidewall coverage, and patterns are well defined at the bottom of the trenches with the lensed mask.

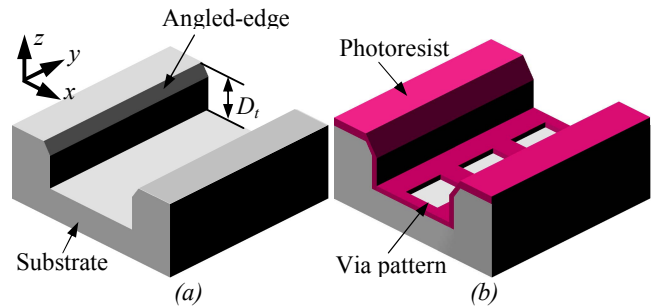


Figure 5: Schematic of the patterning process inside the deep trench; (a) deep vertical trench with angled top-side edges, (b) spray coating and patterning result

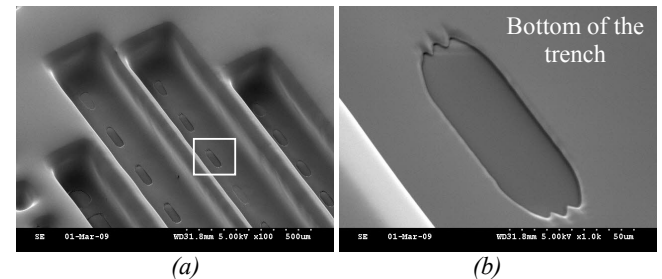


Figure 6: (a) SEM image of the trenches fully covered with patterned spray coated photoresist, (b) magnified view of the rectangle in (a)

As summarized in Table 4, a marked pattern size increase for patterns generated with a conventional mask, and size reduction with decreasing focal length for the lensed mask have been observed. Although the pattern size increase was not significant for proximity exposure on a test wafer without trenches, increased exposure dose ( $1,400\text{mJ}/\text{cm}^2$ ) to accommodate the non-uniformities in photoresist thickness and pattern sizes together with other factors affecting the pattern size, such as sidewall reflection, have resulted in an overall size increase. Exposure dose can be further optimized for better pattern definition, which should be accompanied by the optimization of spray coating process to improve the uniformity of the coated photoresist thickness. However, over-exposure is inevitable in the case of generating

patterns on both the top and bottom surfaces of the trench together by single exposure and development process.

Table 4: Pattern size inside the deep trenches (unit:  $\mu\text{m}$ )

Via Size (Mask)	$50 \times 50 \mu\text{m}^2$	$60 \times 60 \mu\text{m}^2$	$70 \times 70 \mu\text{m}^2$	$80 \times 80 \mu\text{m}^2$
Conventional mask				
Ave. $W_v / H_v$	79.2 / 79.8	90.3 / 88.6		
Mask #1				
Ave. $W_v / H_v$	43.6 / 80.6	67.4 / 86.0		
Mask #2				
Ave. $W_v / H_v$	36.1 / 75.4	28.3 / 90.9		

As summarized in Table 4, the width ( $W_v$ ) and height ( $H_v$ ) of the generated patterns were measured at five different points and averaged to correlate the size reduction with focal length variation from  $267 \mu\text{m}$  to  $459 \mu\text{m}$ . Slight variations in pattern height ( $H_v$ ) can be ascribed to the non-uniformities in the spray coated photoresist thickness. As shown in Figure 7, we have observed a linear relationship between the scaling factor of the pattern width and ratio of the exposure distance to focal depth. The scaling factor of the pattern width has been obtained by dividing the pattern width generated with the lensed mask ( $W_{v,lens}$ ) by that generated with conventional mask ( $W_{v,conventional}$ ). A maximum pattern width reduction of 64%, compared to the pattern generated with conventional mask, has been achieved at the bottom of a  $216 \mu\text{m}$ -deep trench with microlens with focal length of  $267 \mu\text{m}$ .

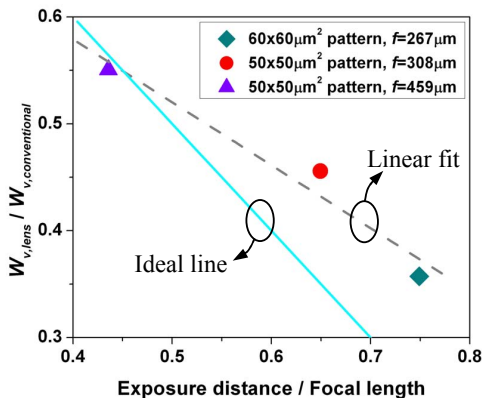


Figure 7: Relationship between scaling factor of the pattern width ( $W_v$ ) and ratio of the exposure distance to focal depth

As shown in Figure 7, assuming an ideal condition for the lens and lithography process, a linear relationship can be estimated between the scaling factor of the pattern width and ratio of the exposure distance to focal depth. Although more information is required to fully account for the non-ideal conditions, current results show that pattern size reduction trends downward as the focal length approaches the exposure distance.

## SUMMARY AND CONCLUSION

A micro projection lithography using a microlens array on a mask has been developed. Microlenses having various focal lengths have been designed and fabricated on a conventional photomask. Deep trenches spray coated with photoresist have been successfully patterned with the lensed mask and the relationship between pattern size variation and focal length of the microlens has been analyzed. The proposed process can be potentially useful for complex three-dimensional structure fabrication as well as for applications where patterning on high topography surfaces is required.

## REFERENCES

- [1] D. S. Tezcan, N. P. Pham, B. Majeed, P. De Moor, W. Ruythooren, K. Baert, "Sloped through wafer vias for 3D wafer level packaging," in *Proc. Elec. Comp. Tech. Conf.*, 2007, pp.643-647.
- [2] C.-H. Ji, F. Herrault, and M. G. Allen, "Metal buried interconnect process for through-wafer interconnection," *J. Micromech. Microeng.*, Vol. 18, 085016 (10pp), 2008.
- [3] N. P. Pham, D. S. Tezcan, W. Ruythooren, P. De Moor, B. Majeed, K. Baert, and B. Swinnen, "Photoresist coating and patterning for through-silicon via technology," *J. Micromech. Microeng.*, Vol. 18, 125008 (9pp), 2008.
- [4] Z. D. Popovic, R. A. Sprague, G. A. Neville Connell, "Technique for monolithic fabrication of microlens array," *Appl. Opt.*, Vol. 27, No. 7, pp. 1281-1284, 1988.
- [5] R. Völkel, H. P. Herzig, P. Nussbaum, R. Dändliker, and W. B. Hügler, "Microlens array imaging system for photolithography," *Opt. Eng.*, Vol. 35, No. 11, pp.3323-3330, 1996.
- [6] M.-H. Wu and G. M. Whitesides, "Fabrication of two-dimensional arrays of microlenses and their applications in photolithography," *J. Micromech. Microeng.*, Vol. 12, pp.747-758, 2002.
- [7] D. Daly, *Microlens Arrays*, Taylor and Francis Inc., New York, 2001.

## CONTACT

\* C.-H. Ji, tel: +1-404-894-8807; cji6@mail.gatech.edu